ELSEVIER

Journal of Power Sources 109 (2002) 333–339

JOURNAL OF POWER SOURCES

www.elsevier.com/locate/jpowsour

Electrochemical properties of $LiM_{1/6}Mn_{11/6}O_4$ (M = Mn, Co, Al and Ni) as cathode materials for Li-ion batteries prepared by ultrasonic spray pyrolysis method

I. Taniguchi*, D. Song, M. Wakihara

Department of Chemical Engineering, Graduate School of Science and Engineering, Tokyo Institute of Technology, 2-12-1 Ookayama, Meguro-ku, Tokyo 152-8552, Japan

Received 25 April 2001; received in revised form 4 February 2002; accepted 7 February 2002

Abstract

Spinel lithium manganese oxide $LiMn_2O_4$ and its substituted forms $LiM_{1/6}Mn_{11/6}O_4$ (M = Co, Al and Ni) were prepared by ultrasonic spray pyrolysis method. As-prepared particles showed a spherical morphology and a densely congested interior structure. The geometric mean diameter was between 0.76 and 0.93 μm, and the geometric standard deviation was approximately 1.33. The crystallite size was approximately 30 nm, and the specific surface area of the particles ranges from 5.7 to 12.7 m^2/g. As-prepared particles were used as cathode active materials for lithium secondary battery and their charge/discharge properties have been investigated. As a result, it could be seen that ultrasonic spray pyrolysis is an effective method to prepare lithium manganese oxide ($LiMn_2O_4$) and its substituted forms within very short production time, which is only 4.8 min in the present work.

Keywords: Spray pyrolysis; Partially substitute spinels; $LiMn_2O_4$; Lithium-ion batteries; Cathode

1. Introduction

The technological advancement in the area of electronics and the onset of electric vehicles necessitate low cost, environment friendly and high energy density lithium-ion batteries. As a part of these requirements, lithium manganese oxide ($LiMn_2O_4$) is considered to be more attractive cathode material for lithium-ion batteries than the competitors such as lithium cobalt or lithium nickel oxides, because of low cost, and acceptable environmental characteristics [1–5]. Unfortunately, $LiMn_2O_4$ can exhibit significant capacity fading during charge/discharge cycle [6–8]. The reason for capacity fading is supposed to be linked to some possible factors, such as: (i) the fracture of structure due to repeated cycle; (ii) decomposition of the electrolyte at high-voltage region; (iii) the dissolution of Mn^{3+} ions into the electrolyte [1]. Many researchers have paid much attention on how to suppress the capacity loss of $LiMn_2O_4$ during cycling [1,7,9]. In our previous investigations, it has been reported that the substituted manganese spinel compounds $LiM_yMn_{2-y}O_4$ (M = Co, Ni, Cr, and Al) have been prepared by solid state reaction and improved in cycle performance significantly comparing with that of parent $LiMn_2O_4$ [10,11]. The good cycle performance has been explained by the relatively stronger metal–oxygen bonding in the substituted spinel than that in $LiMn_2O_4$ [10–12].

It should be noted that the lithium manganese oxide is usually made by solid state reactions, which involves the mechanical mixing of oxides and/or carbonates. These reactions usually require a long firing time and several grinding during the heating process, and moreover, it is difficult to control the particle size of the product. In recent years, there has been considerable interest in producing materials with various powder morphology, bulk density, and stoichiometry by the liquid-phase reaction [13,14]. It is well known that the sol–gel technique has been widely used for a homogeneous process. However, sol–gel method for preparing $LiMn_2O_4$ is also not an economical one because it involves long heating time and complex synthesis process to get the final powder.

Ultrasonic spray pyrolysis is thought to be an effective production technique to lead to short production time, homogenous particle composition and one-step production method [15]. Comparing with the particles prepared by solid state reaction, the particle size distribution is narrow and controllable from micrometer to submicrometer, the purity

* Corresponding author. Tel.: +81-3-5734-2155; fax: +81-3-5734-2155.
E-mail address: itaniguc@chemeng.titech.ac.jp (I. Taniguchi).

0378-7753/02/$ – see front matter
PII: S0378-7753(02)00076-9

of the products is high and it is easy to control the composition and morphology of powders. Recently, it has been reported by Ogihara et al. that they have prepared $LiCoO_2$ and Mg-substituted lithium manganese spinel by this method, and the electrochemical properties has been investigated as well [16,17]. Our group prepared $LiMn_2O_4$ by changing various synthesis factors such as pyrolysis temperature, gas flow rate and initial concentration of precursor solution, and investigated the effect of synthesis conditions on the particle characteristics [18,19].

In this work, $LiMn_2O_4$ and its substituted forms spinel $LiM_{1/6}Mn_{11/6}O_4$ (M = Co, Al and Ni) have been prepared by the ultrasonic spray pyrolysis method. The particle characteristics, such as crystallite size, specific surface area and particle size etc. and electrochemical properties of these compounds have been also investigated.

2. Experimental

2.1. Experimental apparatus

$LiMn_2O_4$ and its substituted forms, such as $LiM_{1/6}Mn_{11/6}O_4$(M = Co, Al and Ni) were prepared by the ultrasonic spray pyrolysis method. The schematic diagram of the experimental apparatus is shown in Fig. 1. This apparatus is divided into three parts such as droplet generator, pyrolysis reactor and particle collector. The droplet generator consists of an ultrasonic nebulizer (1.7 MHz, Omuron Co. Ltd., model NE-U12), a peristaltic pump for supplying precursor solution to the ultrasonic nebulizer and thermostat circulation parts. The pyrolysis reaction tube is formed by putting a quartz glass tube (90 mm i.d., length 1860 mm) into a horizontal electric furnace, which is divided, by five heating zones, and the firing temperature of each zone can be controlled independently. The effective heating length of reaction tube is 1500 mm.

2.2. Sample preparation

$LiMn_2O_4$ and $LiM_{1/6}Mn_{11/6}O_4$ (M = Co, Al and Ni) powders were prepared by using $LiNO_3$, $Mn(NO_3)_2{\cdot}6H_2O$, $Co(NO_3)_2$, $Al(NO_3)_3{\cdot}9H_2O$ and $Ni(NO_3)_2{\cdot}6H_2O$ (Wako Pure Chemical Industries Ltd.) as starting materials. Metal nitrates were measured with atomic ratio (Li:Mn = 1:2 or Li:M:Mn = 1:1/6:11/6) and dissolved in a distilled water. The concentration of the total metal nitrate was 0.45 mol/dm^3. The mist of aqueous nitrate solution was generated by an ultrasonic vibrator, and then the mist was introduced into the electrical furnace to possess a drying and pyrolysis process. The flow rate of the air for carrying the mist was 2 dm^3/min. The mist was remained inside the reaction tube for approximately 4.8 min and pyrolyzed at 1073 K. As-prepared powders were collected using the electrostatic precipitator [20]. The production rate of the sample is 0.5 g/h.

2.3. Characterization

The particle size distribution, geometric mean diameter, morphology and microstructure of particles were determined using a scanning electron microscope (SEM, Hitachi Co., model S-800S). The phase identification of the products was carried out by using powder X-ray diffraction (XRD,

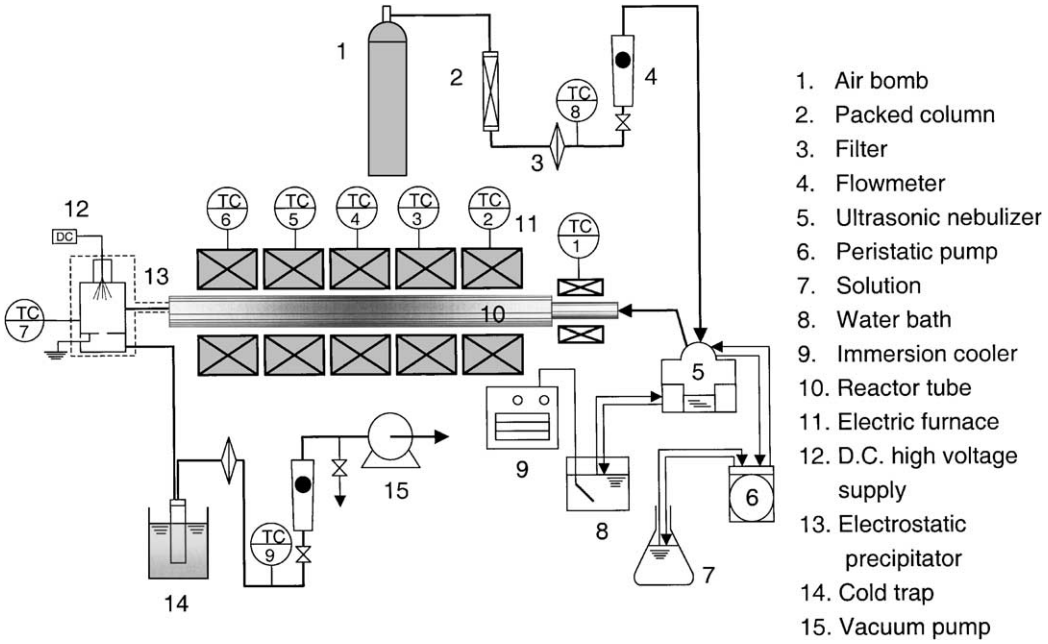

Fig. 1. Schematic diagram of experimental apparatus.

model Rint-2500 V, Rigaku Co. Ltd.). Crystallite size of the as-prepared particles was calculated by Scherrer's equation,

$$d = \frac{0.9\lambda}{(H - h)\cos\theta} \quad (1)$$

where λ is the average value of Cu Kα1 and Cu Kα2; H the full width at half maximum; h the correction constant. The chemical composition of as-prepared powders was determined by inductively coupled plasma spectroscopy (ICP, Seiko, model SPS 1500 VR). The interior structure of as-prepared particles was observed by using TEM (Philip, model EDAXV 99001).

The specific surface area of as-prepared particles was measured by BET method (Shimadzu Co., Flowsorb II 2300). The weight of particles for measurements were approximately 150–200 mg and the samples were dried in vacuum oven for one night before measuring.

2.4. Fabrication and electrochemical characterization

Cathodes were prepared using 75 wt.% $LiM_{1/6}Mn_{11/6}O_4$(M = Co, Al, Ni) powders, 20 wt.% acetylene black and 5 wt.% polytetrafluoroethylene (PTFE), and then made into a thin film. A disk was cut off from the thin film and used as the cathode (5.4 mm diam, ca.). A typical weight of the cathode was 2–3 mg. [1]

A lithium rechargeable cell consists of the cathode, Li foil as an anode, a cellgard microporous membrane as the separator, and 1 mol/dm^3 $LiClO_4$ dissolved in propylene carbonate (PC) (< 20 ppm H_2O, Tomiyama Pure Chemical Co. Ltd.) as the electrolyte. The procedures for the fabrication and the measurements of lithium rechargeable cells are almost the same as those described previously [21].

The cell performance was evaluated by using a potentiostat (Hokuto Denko, model HJR-110mSM6) at current densities of 0.2 and 0.5 mA/cm^2 at room temperature. The cutoff voltage of cycle was between 4.4 and 3.5 V. All of the charge/discharge measurements were carried out inside an argon-filled glove box.

3. Results and discussion

The powder XRD patterns of $LiMn_2O_4$ and $LiM_{1/6}Mn_{11/6}O_4$ (M = Co, Al and Ni) prepared by ultrasonic spray pyrolysis technique are shown in Fig. 2. All samples prepared at 1073 K were identified as a single-phase spinel with a space group $Fd\bar{3}m$ in which the lithium ions occupy the tetrahedral (8a) sites and manganese and substituting metal ions reside at the octahedral (16d) sites.

Table 1 shows the chemical composition of $LiMn_2O_4$ and $LiM_{1/6}Mn_{11/6}O_4$ (M = Co, Al and Ni) powders determined by ICP analysis. The results showed that the chemical composition of all of the as-prepared powders were nearly equal to the stoichiometric ratio as decided.

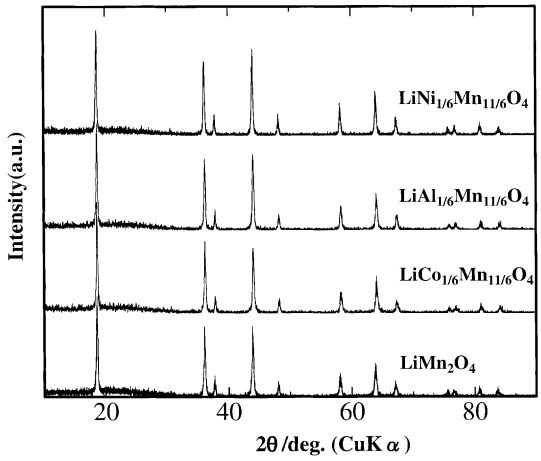

Fig. 2. XRD patterns of $LiMn_2O_4$ and $LiM_{1/6}Mn_{11/6}O_4$(M = Co, Al and Ni).

Table 1
Chemical composition of $LiMn_2O_4$ and $LiM_{1/6}Mn_{11/6}O_4$ (M = Co, Al and Ni)

Sample	Chemical composition		
	Li	M	Mn
$LiMn_2O_4$	1	0	2.040
$LiCo_{1/6}Mn_{11/6}O_4$	1	0.172	1.857
$LiAl_{1/6}Mn_{11/6}O_4$	1	0.165	1.870
$LiNi_{1/6}Mn_{11/6}O_4$	1	0.171	1.867

Typical SEM photographs of $LiMn_2O_4$ and the substituted series $LiM_{1/6}Mn_{11/6}O_4$ (M = Co, Al and Ni) prepared by the ultrasonic spray pyrolysis technique are shown in Fig. 3. All of the as-prepared particles had a spherical morphology and were non-agglomerated. From the SEM photographs, $LiMn_2O_4$ particles showed a clear porous microstructure, but the substituted spinel $LiCo_{1/6}Mn_{11/6}O_4$ and $LiNi_{1/6}Mn_{11/6}O_4$ powders showed an extremely smooth surface appearance. $LiAl_{1/6}Mn_{11/6}O_4$ particles are also microporous structure on the surface appearance. Despite of the same process condition, the surface morphology change takes place by varying the substituted metal of $LiM_{1/6}Mn_{11/6}O_4$.

From SEM photographs, 350 particles were selected randomly from each of the sample, and the particle size of them has been measured. The results for the particle size distributions of $LiMn_2O_4$ and $LiAl_{1/6}Mn_{11/6}O_4$ samples are shown in Fig. 4a and b, respectively. The geometric mean diameters of all samples are also given in Table 2. The geometric standard deviations were approximately around 1.33. It can be seen that the powder has nearly uniform size distribution, and the geometric mean diameter for the as-prepared powders ranges from 0.76 to 0.93 μm. Comparing with the substituted sample $LiM_{1/6}Mn_{11/6}O_4$ (M = Co, Al and Ni), $LiMn_2O_4$ showed a slightly larger particle size value.

[1] The accuracy of balance is within ±0.05 mg.

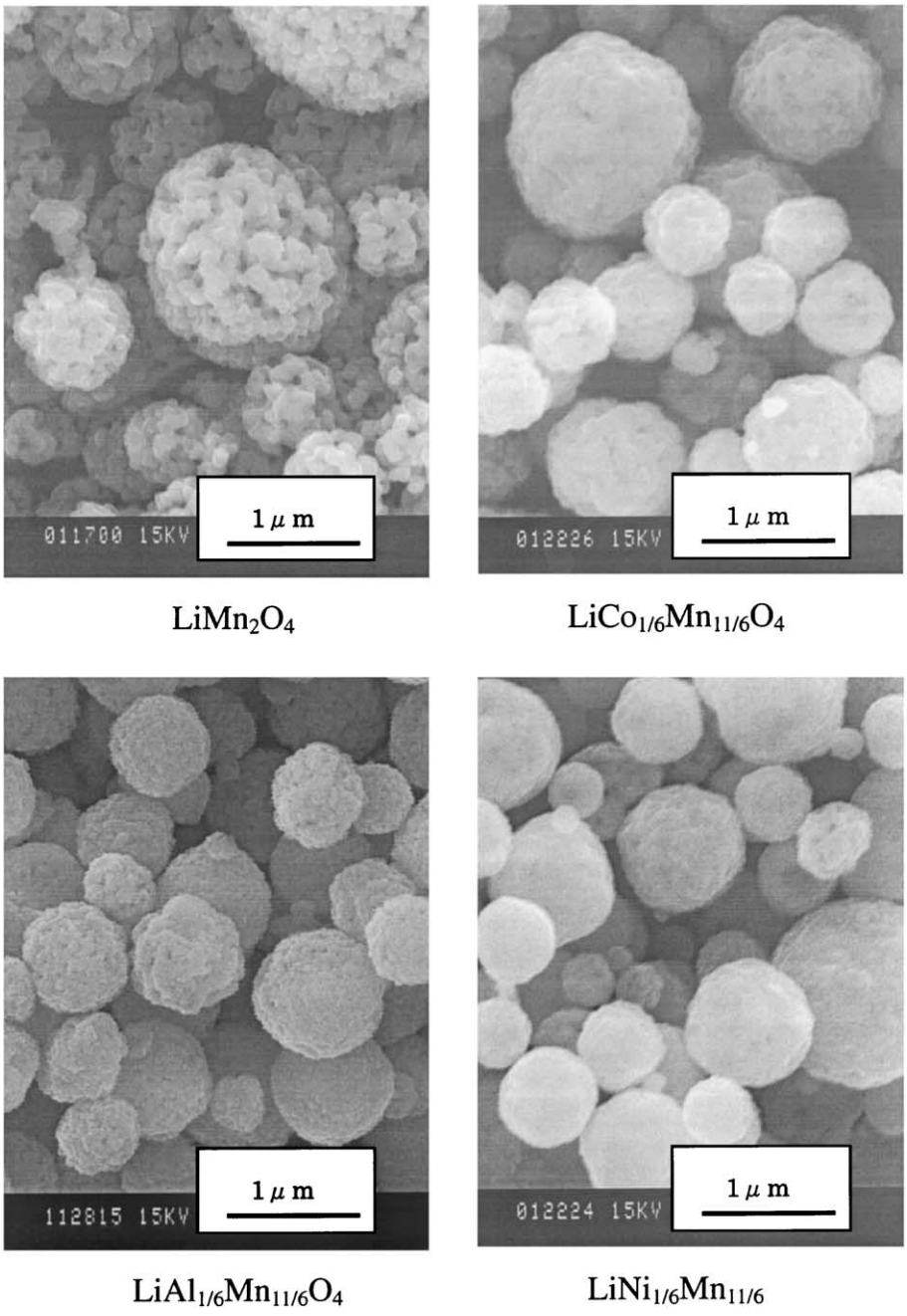

$LiMn_2O_4$ $LiCo_{1/6}Mn_{11/6}O_4$

$LiAl_{1/6}Mn_{11/6}O_4$ $LiNi_{1/6}Mn_{11/6}$

Fig. 3. Surface morphology of $LiMn_2O_4$ and $LiM_{1/6}Mn_{11/6}O_4$(M = Co, Al and Ni) powders.

Table 2
Particle properties of $LiMn_2O_4$ and $LiM_{1/6}Mn_{11/6}O_4$ (M = Co, Al and Ni)

Sample	Geometric mean diameter (μm)	Geometric standard deviation (σ_g)	Specific surface area (m^2/g)	Crystallite size (nm)
$LiMn_2O_4$	0.93	1.33	8.5	33.1
$LiAl_{1/6}Mn_{11/6}O_4$	0.81	1.32	12.7	30.4
$LiNi_{1/6}Mn_{11/6}O_4$	0.76	1.36	5.7	28.0
$LiCo_{1/6}Mn_{11/6}O_4$	0.79	1.33	7.3	30.4

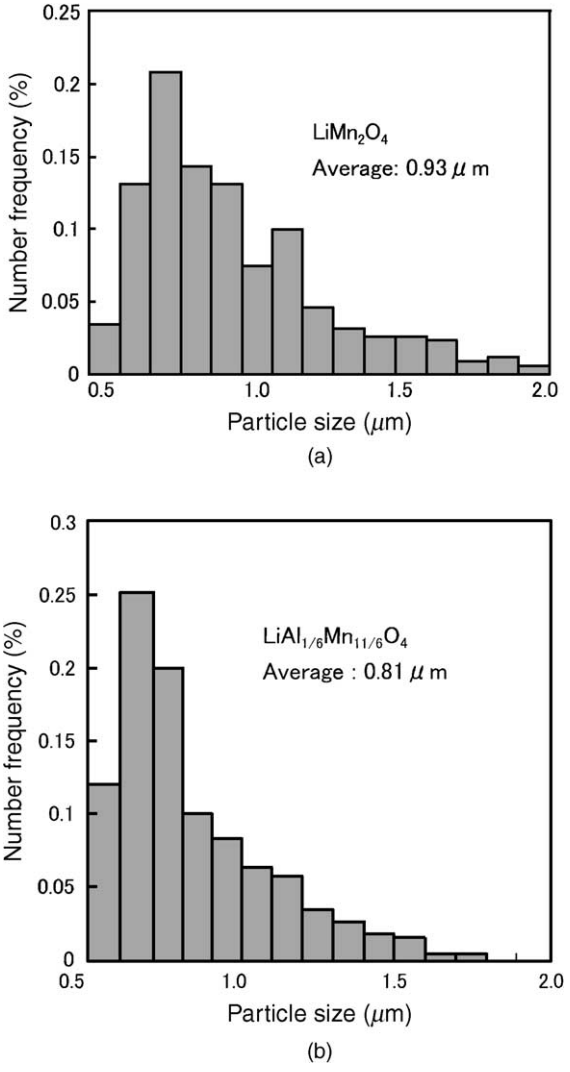

Fig. 4. Particle size distributions of (a) $LiMn_2O_4$ and (b) $LiAl_{1/6}Mn_{11/6}O_4$ powder.

The crystallite size and specific surface area of $LiMn_2O_4$ and $LiM_{1/6}Mn_{11/6}O_4$(M = Al, Co, Ni) powders are summarized in Table 2. The crystalline size was calculated from the XRD pattern by using Scherrer's equation. Calculation was done by using the XRD peak of crystallite plane (4 0 0). The crystallite size for all of samples prepared in this work was approximately 30 nm. This crystallite size fairly agreed with the primary particle size value estimated from the TEM photograph. The specific surface area for all the samples was measured by BET method. The specific surface area of $LiMn_2O_4$ and $LiM_{1/6}Mn_{11/6}O_4$ powders range from 5 to 12 m^2/g. In spite of the same synthesis condition, it led to the change of specific surface area by varying the substituting metal. The specific surface area of $LiCo_{1/6}Mn_{11/6}O_4$ and $LiNi_{1/6}Mn_{11/6}O_4$ powders are lower than the one for $LiMn_2O_4$ due to their smooth surface appearance, however the specific surface area of $LiAl_{1/6}Mn_{11/6}O_4$ is lager than the one of $LiMn_2O_4$. The reason may be due to the fact that the surface morphology of $LiAl_{1/6}Mn_{11/6}O_4$ shows a microporous

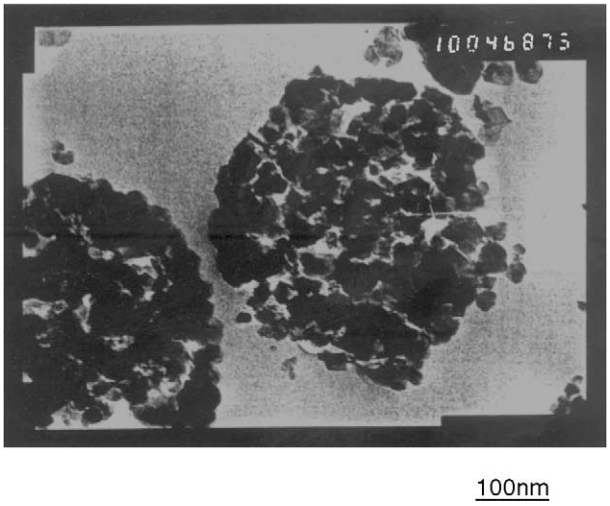

Fig. 5. TEM photograph of a $LiAl_{1/6}Mn_{11/6}O_4$ particle.

structure, the diameter is smaller than the one of $LiMn_2O_4$ and, moreover, aluminum is a light metal in comparison with manganese.

Fig. 5 shows the TEM photograph of $LiAl_{1/6}Mn_{11/6}O_4$ particle. It can be clearly seen that the particle prepared at 1073 K with a 2 dm^3/min carrier gas flow rate is consisted by the cohesion of the primary particles. From the TEM photograph, it can be estimated that the primary particle size was approximately a few ten nanometer.

Fig. 6 shows the first charge–discharge curves of Li|$LiM_{1/6}Mn_{11/6}O_4$ cells for M = Co, Al and Ni together with that of the Li|$LiMn_2O_4$ cell. It can be seen obviously that the charge/discharge curves of all of the samples had two voltage plateaus at approximately 4.05 and 4.1 V, which is a remarkable characteristic of a well-defined $LiMn_2O_4$ spinel. From charge/discharge curves, it is found that lithium ion was reversibly lithiated/delithiated through $LiMn_2O_4$ spinel framework.

The initial capacity of the cells decreased by substituting a part of manganese by Co, Al and Ni. The initial capacity of

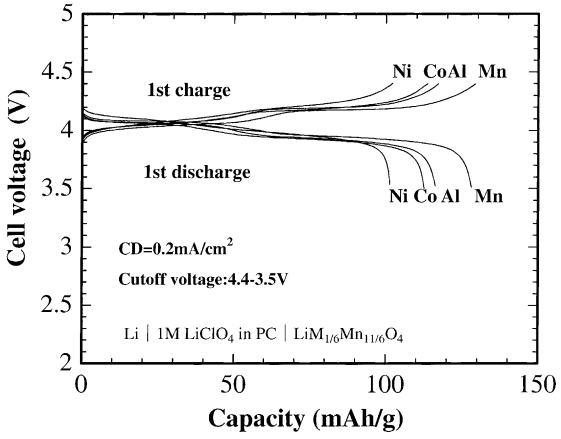

Fig. 6. Charge/discharge curves of Li|$LiMn_2O_4$ and Li|$LiM_{1/6}Mn_{11/6}O_4$ (M = Co, Al and Ni) cells at first cycle.

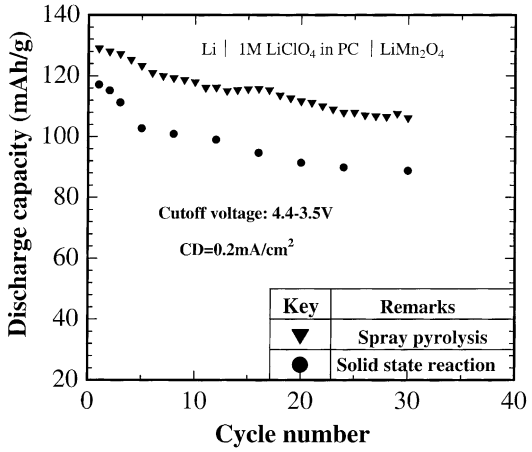

Fig. 7. Cycle performance of Li|$LiMn_2O_4$ prepared by spray pyrolysis method and solid-state reaction method cell.

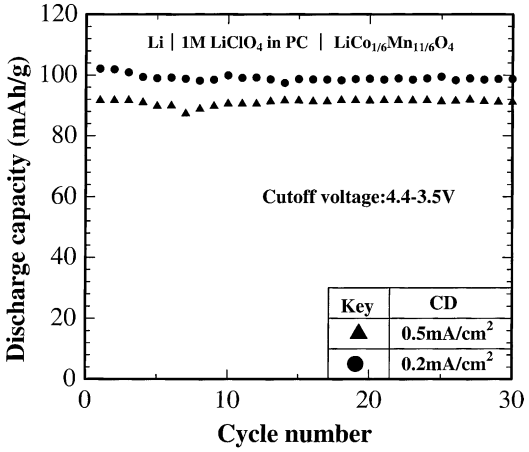

Fig. 9. Cycle performance of Li|$LiCo_{1/6}Mn_{11/6}O_4$ cell at 0.2 and 0.5 mA/cm^2, respectively.

Li|$LiMn_2O_4$ cell obtained in this work was 129 mAh/g (theoretical capacity of $LiMn_2O_4$ is 148 mAh/g). By substituting with Al, Co and Ni, the initial capacity decreased to 117, 113 and 101 mAh/g, respectively. This is due to the decrease of Mn^{3+} amount in $LiMn_2O_4$ since only the amount of Mn^{3+} contributes to the charge/discharge capacity. Among the substituting spinel, the nickel-substituted cathode showed the lowest initial capacity because of the much decrease of Mn^{3+} amount. Comparing with that of prepared by solid state reaction technique [10], the initial capacity of $LiMn_2O_4$ prepared by spray pyrolysis increased to some extent.

Fig. 7 shows the comparison of the cycle performance of $LiMn_2O_4$ powder, which prepared by solid-state reaction and ultrasonic spray pyrolysis, respectively. The capacity retention rate which the discharge capacity at 30th cycle is normalized by the initial one was about 75% for the solid state reaction sample. However, for the sample prepared by ultrasonic spray pyrolysis method, the capacity retention rate increased up to 85%. The fact may indicate that the spherical particle morphology, homogenous particle composition and narrow distribution of particle size have a good effect on the improvement of cycle performance.

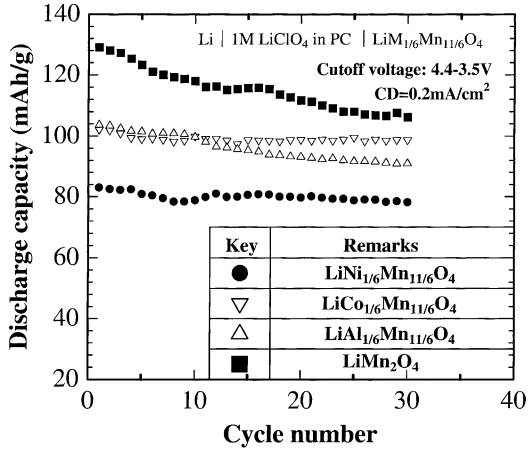

Fig. 8. Cycle performance of Li|$LiMn_2O_4$ and Li|$LiM_{1/6}Mn_{11/6}O_4$(M = Co, Al and Ni).

Fig. 8 shows the cycle performance of the Li|$LiM_{1/6}Mn_{11/6}O_4$ cell over subsequent cycles for M = Al, Co and Ni, respectively. Comparing with the poor cycle performance occurred with $LiMn_2O_4$ cathode, the substituted spinel exhibited a remarkable improvement of cycle behavior. Especially for Co and Ni-substituted spinel cathode, after 30 times charge/discharge cycle, the capacity loss of $LiCo_{1/6}Mn_{11/6}O_4$ sample was only 2%, and the $LiNi_{1/6}Mn_{11/6}O_4$ sample was less than 4%. The cycle performance of $LiCo_{1/6}Mn_{11/6}O_4$ cathode at current density 0.5 mA/cm^2 is also shown in Fig. 9. The cycle performance is quite similar to the one at 0.2 mA/cm^2, however the capacity slightly decreases with increasing the current density.

4. Conclusions

$LiMn_2O_4$ and $LiM_{1/6}Mn_{11/6}O_4$ (M = Co, Al and Ni) were prepared by using ultrasonic spray pyrolysis method. All of the as-prepared powders were identified as a single spinel phase with $Fd\bar{3}m$ space group. The powders had a spherical morphology and densely congested interior structure. The first discharge capacity of $LiMn_2O_4$ was 129 mAh/g at 0.2 mA/cm^2, and the cycle performance was more stable than that of prepared by solid state reaction. The substituted spinels $LiM_{1/6}Mn_{11/6}O_4$ (M = Co, Al and Ni) showed a good cycle life as well. Especially for $LiCo_{1/6}Mn_{11/6}O_4$, the capacity loss was only 2% after 30 cycles. Thus, it can be seen that ultrasonic spray pyrolysis is an effective method to prepare lithium manganese oxide $LiMn_2O_4$ and its substituted forms within very short reaction time. Comparing with solid state reaction, it makes possible to obtain particles with homogeneous composition and good electrochemical properties within short production time and simple process.

Acknowledgements

This research work has been partially supported by the Suzuki Foundation and the Hosokawa Powder Technology Foundation.

References

[1] J.M. Tarascon, E. Wang, F.K. Shokoohi, W.R. McKinnon, S. Colson, J. Electrochem. Soc. 138 (1991) 2859.
[2] T. Ohzuku, M. Kitagawa, T. Hirai, J. Electrochem. Soc. 137 (1990) 769.
[3] J.M. Tarascon, D. Guyomard, Electrochim. Acta 38 (1993) 1221.
[4] G. Pistoia, G. Wang, C. Wang, Solid State Ionics 58 (1992) 285.
[5] H. Huang, P.G. Bruce, J. Power Sources 54 (1995) 52.
[6] J.M. Tarascon, W.R. McKinnon, F. Coowar, T.N. Bowmer, G. Amatucci, D. Guyomard, J. Electrochem. Soc. 141 (1994) 1421.
[7] R.J. Gummow, A. de Kock, M.M. Thackeray, Solid State Ionics 69 (1994) 59.
[8] Y. Xia, H. Noguchi, M. Yoshio, J. Solid State Chem. 119 (1995) 216.
[9] R. Bittihn, R. Herr, D. Hoge, J. Power Sources 43/44 (1993) 223.
[10] L. Guohua, H. Ikuta, T. Uchida, M. Wakihara, J. Electrochem. Soc. 143 (1996) 178.
[11] D. Song, H. Ikuta, T. Uchida, M. Wakihara, Solid State Ionics 117 (1999) 151.
[12] M. Wakihara, G. Li, H. Ikuta, in: M. Wakihara, O. Yamamoto (Eds.), Lithium Ion Batteries, Kodansha, Tokyo, 1998, p. 26.
[13] X. Qiu, X. Sun, W. Shen, N. Chen, Solid State Ionics 93 (1997) 335.
[14] H. Huang, P.G. Bruce, J. Electrochem. Soc. 141 (1994) L106.
[15] G.L. Messing, S.C. Zhang, G.V. Javanthi, J. Am. Ceram. Soc. 76 (1993) 2707.
[16] T. Ogihara, Y. Saito, T. Yanagawa, N. Ogata, K. Yoshida, K. Ogawa, J. Ceram. Soc. Jpn. 101 (1993) 1159.
[17] T. Ogihara, N. Ogata, K. Katayama, Y. Azuma, N. Mizutani, Electrochemistry 68 (2000) 162.
[18] I. Taniguchi, C.K. Lim, Kagaku Kogaku Ronbunshu 27 (2001) 93.
[19] I. Taniguchi, C. K. Lim, Y. Negishi, in: The Proceedings of Chemical and Process Engineering Conference (CPEC) 2000, Singapore, in conjunction with Regional Symposium on Chemical Engineering (RSCE) 2000, RE1.2.
[20] K. Okuyama, M. Shimada, M. Adachi, N. Tohge, J. Aerosol Sci. 24 (1993) 357.
[21] M. Wakihara, T. Uchida, K. Suzuki, M. Taniguchi, Electrochim. Acta 34 (1989) 867.